

Measurement of the Ratios of Branching Fractions

$$\mathcal{B}(B_s^0 \rightarrow D_s^- \pi^+ \pi^+ \pi^-) / \mathcal{B}(B^0 \rightarrow D^- \pi^+ \pi^+ \pi^-) \text{ and } \mathcal{B}(B_s^0 \rightarrow D_s^- \pi^+) / \mathcal{B}(B^0 \rightarrow D^- \pi^+)$$

A. Abulencia,²³ J. Adelman,¹³ T. Affolder,¹⁰ T. Akimoto,⁵⁵ M.G. Albrow,¹⁶ D. Ambrose,¹⁶ S. Amerio,⁴³ D. Amidei,³⁴ A. Anastassov,⁵² K. Anikeev,¹⁶ A. Annovi,¹⁸ J. Antos,¹ M. Aoki,⁵⁵ G. Apollinari,¹⁶ J.-F. Arguin,³³ T. Arisawa,⁵⁷ A. Artikov,¹⁴ W. Ashmanskas,¹⁶ A. Attal,⁸ F. Azfar,⁴² P. Azzi-Bacchetta,⁴³ P. Azzurri,⁴⁶ N. Bacchetta,⁴³ W. Badgett,¹⁶ A. Barbaro-Galtieri,²⁸ V.E. Barnes,⁴⁸ B.A. Barnett,²⁴ S. Baroiant,⁷ V. Bartsch,³⁰ G. Bauer,³² F. Bedeschi,⁴⁶ S. Behari,²⁴ S. Belforte,⁵⁴ G. Bellettini,⁴⁶ J. Bellinger,⁵⁹ A. Belloni,³² D. Benjamin,¹⁵ A. Beretvas,¹⁶ J. Beringer,²⁸ T. Berry,²⁹ A. Bhatti,⁵⁰ M. Binkley,¹⁶ D. Bisello,⁴³ R.E. Blair,² C. Blocker,⁶ B. Blumenfeld,²⁴ A. Bocci,¹⁵ A. Bodek,⁴⁹ V. Boisvert,⁴⁹ G. Bolla,⁴⁸ A. Bolshov,³² D. Bortoletto,⁴⁸ J. Boudreau,⁴⁷ A. Boveia,¹⁰ B. Brau,¹⁰ L. Brigliadori,⁵ C. Bromberg,³⁵ E. Brubaker,¹³ J. Budagov,¹⁴ H.S. Budd,⁴⁹ S. Budd,²³ S. Budroni,⁴⁶ K. Burkett,¹⁶ G. Busetto,⁴³ P. Bussey,²⁰ K. L. Byrum,² S. Cabrera,¹⁵ M. Campanelli,¹⁹ M. Campbell,³⁴ F. Canelli,¹⁶ A. Canepa,⁴⁸ S. Carillo,¹⁷ D. Carlsmith,⁵⁹ R. Carosi,⁴⁶ M. Casarsa,⁵⁴ A. Castro,⁵ P. Catastini,⁴⁶ D. Cauz,⁵⁴ M. Cavalli-Sforza,³ A. Cerri,²⁸ L. Cerrito,⁴² S.H. Chang,²⁷ Y.C. Chen,¹ M. Chertok,⁷ G. Chiarelli,⁴⁶ G. Chlachidze,¹⁴ F. Chlebana,¹⁶ I. Cho,²⁷ K. Cho,²⁷ D. Chokheli,¹⁴ J.P. Chou,²¹ G. Choudalakis,³² S.H. Chuang,⁵⁹ K. Chung,¹² W.H. Chung,⁵⁹ Y.S. Chung,⁴⁹ M. Ciljak,⁴⁶ C.I. Ciobanu,²³ M.A. Ciocci,⁴⁶ A. Clark,¹⁹ D. Clark,⁶ M. Coca,¹⁵ G. Compostella,⁴³ M.E. Convery,⁵⁰ J. Conway,⁷ B. Cooper,³⁵ K. Copic,³⁴ M. Cordelli,¹⁸ G. Cortiana,⁴³ F. Crescioli,⁴⁶ C. Cuenca Almenar,⁷ J. Cuevas,¹¹ R. Culbertson,¹⁶ J.C. Cully,³⁴ D. Cyr,⁵⁹ S. DaRonco,⁴³ S. D'Auria,²⁰ T. Davies,²⁰ M. D'Onofrio,³ D. Dagenhart,⁶ P. de Barbaro,⁴⁹ S. De Cecco,⁵¹ A. Deisher,²⁸ G. De Lentdecker,⁴⁹ M. Dell'Orso,⁴⁶ F. Delli Paoli,⁴³ L. Demortier,⁵⁰ J. Deng,¹⁵ M. Deninno,⁵ D. De Pedis,⁵¹ P.F. Derwent,¹⁶ G.P. Di Giovanni,⁴⁴ C. Dionisi,⁵¹ B. Di Ruzza,⁵⁴ J.R. Dittmann,⁴ P. DiTuro,⁵² C. Dörr,²⁵ S. Donati,⁴⁶ M. Donega,¹⁹ P. Dong,⁸ J. Donini,⁴³ T. Dorigo,⁴³ S. Dube,⁵² J. Efron,³⁹ R. Erbacher,⁷ D. Errede,²³ S. Errede,²³ R. Eusebi,¹⁶ H.C. Fang,²⁸ S. Farrington,²⁹ I. Fedorko,⁴⁶ W.T. Fedorko,¹³ R.G. Feild,⁶⁰ M. Feindt,²⁵ J.P. Fernandez,³¹ R. Field,¹⁷ G. Flanagan,⁴⁸ A. Foland,²¹ S. Forrester,⁷ G.W. Foster,¹⁶ M. Franklin,²¹ J.C. Freeman,²⁸ I. Furic,¹³ M. Gallinaro,⁵⁰ J. Galyardt,¹² J.E. Garcia,⁴⁶ F. Garberon,¹⁰ A.F. Garfinkel,⁴⁸ C. Gay,⁶⁰ H. Gerberich,²³ D. Gerdes,³⁴ S. Giagu,⁵¹ P. Giannetti,⁴⁶ A. Gibson,²⁸ K. Gibson,⁴⁷ J.L. Gimmell,⁴⁹ C. Ginsburg,¹⁶ N. Giokaris,¹⁴ M. Giordani,⁵⁴ P. Giromini,¹⁸ M. Giunta,⁴⁶ G. Giurgiu,¹² V. Glagolev,¹⁴ D. Glenzinski,¹⁶ M. Gold,³⁷ N. Goldschmidt,¹⁷ J. Goldstein,⁴² G. Gomez,¹¹ G. Gomez-Ceballos,¹¹ M. Goncharov,⁵³ O. González,³¹ I. Gorelov,³⁷ A.T. Goshaw,¹⁵ K. Goulios,⁵⁰ A. Gresele,⁴³ M. Griffiths,²⁹ S. Grinstein,²¹ C. Grosso-Pilcher,¹³ R.C. Group,¹⁷ U. Grundler,²³ J. Guimaraes da Costa,²¹ Z. Gunay-Unalan,³⁵ C. Haber,²⁸ K. Hahn,³² S.R. Hahn,¹⁶ E. Halkiadakis,⁵² A. Hamilton,³³ B.-Y. Han,⁴⁹ J.Y. Han,⁴⁹ R. Handler,⁵⁹ F. Happacher,¹⁸ K. Hara,⁵⁵ M. Hare,⁵⁶ S. Harper,⁴² R.F. Harr,⁵⁸ R.M. Harris,¹⁶ M. Hartz,⁴⁷ K. Hatakeyama,⁵⁰ J. Hauser,⁸ A. Heijboer,⁴⁵ B. Heinemann,²⁹ J. Heinrich,⁴⁵ C. Henderson,³² M. Herndon,⁵⁹ J. Heuser,²⁵ D. Hidas,¹⁵ C.S. Hill,¹⁰ D. Hirschbuehl,²⁵ A. Hocker,¹⁶ A. Holloway,²¹ S. Hou,¹ M. Houlden,²⁹ S.-C. Hsu,⁹ B.T. Huffman,⁴² R.E. Hughes,³⁹ U. Husemann,⁶⁰ J. Huston,³⁵ J. Incandela,¹⁰ G. Introzzi,⁴⁶ M. Iori,⁵¹ Y. Ishizawa,⁵⁵ A. Ivanov,⁷ B. Iyutin,³² E. James,¹⁶ D. Jang,⁵² B. Jayatilaka,³⁴ D. Jeans,⁵¹ H. Jensen,¹⁶ E.J. Jeon,²⁷ S. Jindariani,¹⁷ M. Jones,⁴⁸ K.K. Joo,²⁷ S.Y. Jun,¹² J.E. Jung,²⁷ T.R. Junk,²³ T. Kamon,⁵³ P.E. Karchin,⁵⁸ Y. Kato,⁴¹ Y. Kemp,²⁵ R. Kephart,¹⁶ U. Kerzel,²⁵ V. Khotilovich,⁵³ B. Kilminster,³⁹ D.H. Kim,²⁷ H.S. Kim,²⁷ J.E. Kim,²⁷ M.J. Kim,¹² S.B. Kim,²⁷ S.H. Kim,⁵⁵ Y.K. Kim,¹³ N. Kimura,⁵⁵ L. Kirsch,⁶ S. Klimenko,¹⁷ M. Klute,³² B. Knuteson,³² B.R. Ko,¹⁵ K. Kondo,⁵⁷ D.J. Kong,²⁷ J. Konigsberg,¹⁷ A. Korytov,¹⁷ A.V. Kotwal,¹⁵ A. Kovalev,⁴⁵ A.C. Kraan,⁴⁵ J. Kraus,²³ I. Kravchenko,³² M. Kreps,²⁵ J. Kroll,⁴⁵ N. Krumnack,⁴ M. Kruse,¹⁵ V. Krutelyov,¹⁰ T. Kubo,⁵⁵ S. E. Kuhlmann,² T. Kuhr,²⁵ Y. Kusakabe,⁵⁷ S. Kwang,¹³ A.T. Laasanen,⁴⁸ S. Lai,³³ S. Lami,⁴⁶ S. Lammel,¹⁶ M. Lancaster,³⁰ R.L. Lander,⁷ K. Lannon,³⁹ A. Lath,⁵² G. Latino,⁴⁶ I. Lazzizzera,⁴³ T. LeCompte,² J. Lee,⁴⁹ J. Lee,²⁷ Y.J. Lee,²⁷ S.W. Lee,⁵³ R. Lefèvre,³ N. Leonardo,³² S. Leone,⁴⁶ S. Levy,¹³ J.D. Lewis,¹⁶ C. Lin,⁶⁰ C.S. Lin,¹⁶ M. Lindgren,¹⁶ E. Lipeles,⁹ A. Lister,⁷ D.O. Litvintsev,¹⁶ T. Liu,¹⁶ N.S. Lockyer,⁴⁵ A. Loginov,³⁶ M. Loreti,⁴³ P. Loverre,⁵¹ R.-S. Lu,¹ D. Lucchesi,⁴³ P. Lujan,²⁸ P. Lukens,¹⁶ G. Lungu,¹⁷ L. Lyons,⁴² J. Lys,²⁸ R. Lysak,¹ E. Lytken,⁴⁸ P. Mack,²⁵ D. MacQueen,³³ R. Madrak,¹⁶ K. Maeshima,¹⁶ K. Makhoul,³² T. Maki,²² P. Maksimovic,²⁴ S. Malde,⁴² G. Manca,²⁹ F. Margaroli,⁵ R. Marginean,¹⁶ C. Marino,²⁵ C.P. Marino,²³ A. Martin,⁶⁰ M. Martin,²⁰ V. Martin,²⁰ M. Martínez,³ T. Maruyama,⁵⁵ P. Mastrandrea,⁵¹ T. Masubuchi,⁵⁵ H. Matsunaga,⁵⁵ M.E. Mattson,⁵⁸ R. Mazini,³³ P. Mazzanti,⁵ K.S. McFarland,⁴⁹ P. McIntyre,⁵³ R. McNulty,²⁹ A. Mehta,²⁹ P. Mehtala,²² S. Menzemer,¹¹ A. Menzione,⁴⁶ P. Merkel,⁴⁸ C. Mesropian,⁵⁰ A. Messina,³⁵ T. Miao,¹⁶

N. Miladinovic,⁶ J. Miles,³² R. Miller,³⁵ C. Mills,¹⁰ M. Milnik,²⁵ A. Mitra,¹ G. Mitselmakher,¹⁷ A. Miyamoto,²⁶ S. Moed,¹⁹ N. Moggi,⁵ B. Mohr,⁸ R. Moore,¹⁶ M. Morello,⁴⁶ P. Movilla Fernandez,²⁸ J. Müllenstädt,²⁸ A. Mukherjee,¹⁶ Th. Müller,²⁵ R. Mumford,²⁴ P. Murat,¹⁶ J. Nachtman,¹⁶ A. Nagano,⁵⁵ J. Naganoma,⁵⁷ I. Nakano,⁴⁰ A. Napier,⁵⁶ V. Necula,¹⁷ C. Neu,⁴⁵ M.S. Neubauer,⁹ J. Nielsen,²⁸ T. Nigmanov,⁴⁷ L. Nodulman,² O. Norriella,³ E. Nurse,³⁰ S.H. Oh,¹⁵ Y.D. Oh,²⁷ I. Oksuzian,¹⁷ T. Okusawa,⁴¹ R. Oldeman,²⁹ R. Orava,²² K. Osterberg,²² C. Pagliarone,⁴⁶ E. Palencia,¹¹ V. Papadimitriou,¹⁶ A.A. Paramonov,¹³ B. Parks,³⁹ S. Pashapour,³³ J. Patrick,¹⁶ G. Pauletta,⁵⁴ M. Paulini,¹² C. Paus,³² D.E. Pellett,⁷ A. Penzo,⁵⁴ T.J. Phillips,¹⁵ G. Piacentino,⁴⁶ J. Piedra,⁴⁴ L. Pinera,¹⁷ K. Pitts,²³ C. Plager,⁸ L. Pondrom,⁵⁹ X. Portell,³ O. Poukhov,¹⁴ N. Pounder,⁴² F. Prakoshyn,¹⁴ A. Pronko,¹⁶ J. Proudfoot,² F. Ptohos,¹⁸ G. Punzi,⁴⁶ J. Pursley,²⁴ J. Rademacker,⁴² A. Rahaman,⁴⁷ N. Ranjan,⁴⁸ S. Rappoccio,²¹ B. Reisert,¹⁶ V. Rekovic,³⁷ P. Renton,⁴² M. Rescigno,⁵¹ S. Richter,²⁵ F. Rimondi,⁵ L. Ristori,⁴⁶ A. Robson,²⁰ T. Rodrigo,¹¹ E. Rogers,²³ S. Rolli,⁵⁶ R. Roser,¹⁶ M. Rossi,⁵⁴ R. Rossin,¹⁷ A. Ruiz,¹¹ J. Russ,¹² V. Rusu,¹³ H. Saarikko,²² S. Sabik,³³ A. Safonov,⁵³ W.K. Sakumoto,⁴⁹ G. Salamanna,⁵¹ O. Saltó,³ D. Saltzberg,⁸ C. Sánchez,³ L. Santi,⁵⁴ S. Sarkar,⁵¹ L. Sartori,⁴⁶ K. Sato,¹⁶ P. Savard,³³ A. Savoy-Navarro,⁴⁴ T. Scheidle,²⁵ P. Schlabach,¹⁶ E.E. Schmidt,¹⁶ M.P. Schmidt,⁶⁰ M. Schmitt,³⁸ T. Schwarz,⁷ L. Scodellaro,¹¹ A.L. Scott,¹⁰ A. Scribano,⁴⁶ F. Scuri,⁴⁶ A. Sedov,⁴⁸ S. Seidel,³⁷ Y. Seiya,⁴¹ A. Semenov,¹⁴ L. Sexton-Kennedy,¹⁶ A. Sfyrila,¹⁹ M.D. Shapiro,²⁸ T. Shears,²⁹ P.F. Shepard,⁴⁷ D. Sherman,²¹ M. Shimojima,⁵⁵ M. Shochet,¹³ Y. Shon,⁵⁹ I. Shreyber,³⁶ A. Sidoti,⁴⁶ P. Sinervo,³³ A. Sisakyan,¹⁴ J. Sjolin,⁴² A.J. Slaughter,¹⁶ J. Slaunwhite,³⁹ K. Sliwa,⁵⁶ J.R. Smith,⁷ F.D. Snider,¹⁶ R. Snihur,³³ M. Soderberg,³⁴ A. Soha,⁷ S. Somalwar,⁵² V. Sorin,³⁵ J. Spalding,¹⁶ F. Spinella,⁴⁶ T. Spreitzer,³³ P. Squillacioti,⁴⁶ M. Stanitzki,⁶⁰ A. Staveris-Polykalas,⁴⁶ R. St. Denis,²⁰ B. Stelzer,⁸ O. Stelzer-Chilton,⁴² D. Stentz,³⁸ J. Strologas,³⁷ D. Stuart,¹⁰ J.S. Suh,²⁷ A. Sukhanov,¹⁷ H. Sun,⁵⁶ T. Suzuki,⁵⁵ A. Taffard,²³ R. Takashima,⁴⁰ Y. Takeuchi,⁵⁵ K. Takikawa,⁵⁵ M. Tanaka,² R. Tanaka,⁴⁰ M. Tecchio,³⁴ P.K. Teng,¹ K. Terashi,⁵⁰ J. Thom,¹⁶ A.S. Thompson,²⁰ E. Thomson,⁴⁵ P. Tipton,⁶⁰ V. Tiwari,¹² S. Tkaczyk,¹⁶ D. Toback,⁵³ S. Tokar,¹⁴ K. Tollefson,³⁵ T. Tomura,⁵⁵ D. Tonelli,⁴⁶ S. Torre,¹⁸ D. Torretta,¹⁶ S. Tourneur,⁴⁴ W. Trischuk,³³ R. Tsuchiya,⁵⁷ S. Tsuno,⁴⁰ N. Turini,⁴⁶ F. Ukegawa,⁵⁵ T. Unverhau,²⁰ S. Uozumi,⁵⁵ D. Usynin,⁴⁵ S. Vallecorsa,¹⁹ N. van Remortel,²² A. Varganov,³⁴ E. Vataga,³⁷ F. Vázquez,¹⁷ G. Velev,¹⁶ G. Veramendi,²³ V. Veszpremi,⁴⁸ R. Vidal,¹⁶ I. Vila,¹¹ R. Vilar,¹¹ T. Vine,³⁰ I. Vollrath,³³ I. Volobouev,²⁸ G. Volpi,⁴⁶ F. Würthwein,⁹ P. Wagner,⁵³ R.G. Wagner,² R.L. Wagner,¹⁶ J. Wagner,²⁵ W. Wagner,²⁵ R. Wallny,⁸ S.M. Wang,¹ A. Warburton,³³ S. Waschke,²⁰ D. Waters,³⁰ W.C. Wester III,¹⁶ B. Whitehouse,⁵⁶ D. Whiteson,⁴⁵ A.B. Wicklund,² E. Wicklund,¹⁶ G. Williams,³³ H.H. Williams,⁴⁵ P. Wilson,¹⁶ B.L. Winer,³⁹ P. Wittich,¹⁶ S. Wolbers,¹⁶ C. Wolfe,¹³ T. Wright,³⁴ X. Wu,¹⁹ S.M. Wynne,²⁹ A. Yagil,¹⁶ K. Yamamoto,⁴¹ J. Yamaoka,⁵² T. Yamashita,⁴⁰ C. Yang,⁶⁰ U.K. Yang,¹³ Y.C. Yang,²⁷ W.M. Yao,²⁸ G.P. Yeh,¹⁶ J. Yoh,¹⁶ K. Yorita,¹³ T. Yoshida,⁴¹ G.B. Yu,⁴⁹ I. Yu,²⁷ S.S. Yu,¹⁶ J.C. Yun,¹⁶ L. Zanello,⁵¹ A. Zanetti,⁵⁴ I. Zaw,²¹ X. Zhang,²³ J. Zhou,⁵² and S. Zucchelli⁵

(CDF Collaboration)

¹*Institute of Physics, Academia Sinica, Taipei, Taiwan 11529, Republic of China*

²*Argonne National Laboratory, Argonne, Illinois 60439*

³*Institut de Fisica d'Altes Energies, Universitat Autònoma de Barcelona, E-08193, Bellaterra (Barcelona), Spain*

⁴*Baylor University, Waco, Texas 76798*

⁵*Istituto Nazionale di Fisica Nucleare, University of Bologna, I-40127 Bologna, Italy*

⁶*Brandeis University, Waltham, Massachusetts 02254*

⁷*University of California, Davis, Davis, California 95616*

⁸*University of California, Los Angeles, Los Angeles, California 90024*

⁹*University of California, San Diego, La Jolla, California 92093*

¹⁰*University of California, Santa Barbara, Santa Barbara, California 93106*

¹¹*Instituto de Fisica de Cantabria, CSIC-University of Cantabria, 39005 Santander, Spain*

¹²*Carnegie Mellon University, Pittsburgh, PA 15213*

¹³*Enrico Fermi Institute, University of Chicago, Chicago, Illinois 60637*

¹⁴*Joint Institute for Nuclear Research, RU-141980 Dubna, Russia*

¹⁵*Duke University, Durham, North Carolina 27708*

¹⁶*Fermi National Accelerator Laboratory, Batavia, Illinois 60510*

¹⁷*University of Florida, Gainesville, Florida 32611*

¹⁸*Laboratori Nazionali di Frascati, Istituto Nazionale di Fisica Nucleare, I-00044 Frascati, Italy*

¹⁹*University of Geneva, CH-1211 Geneva 4, Switzerland*

²⁰*Glasgow University, Glasgow G12 8QQ, United Kingdom*

²¹*Harvard University, Cambridge, Massachusetts 02138*

- ²²*Division of High Energy Physics, Department of Physics, University of Helsinki and Helsinki Institute of Physics, FIN-00014, Helsinki, Finland*
- ²³*University of Illinois, Urbana, Illinois 61801*
- ²⁴*The Johns Hopkins University, Baltimore, Maryland 21218*
- ²⁵*Institut für Experimentelle Kernphysik, Universität Karlsruhe, 76128 Karlsruhe, Germany*
- ²⁶*High Energy Accelerator Research Organization (KEK), Tsukuba, Ibaraki 305, Japan*
- ²⁷*Center for High Energy Physics: Kyungpook National University, Taegu 702-701, Korea; Seoul National University, Seoul 151-742, Korea; and SungKyunKwan University, Suwon 440-746, Korea*
- ²⁸*Ernest Orlando Lawrence Berkeley National Laboratory, Berkeley, California 94720*
- ²⁹*University of Liverpool, Liverpool L69 7ZE, United Kingdom*
- ³⁰*University College London, London WC1E 6BT, United Kingdom*
- ³¹*Centro de Investigaciones Energeticas Medioambientales y Tecnologicas, E-28040 Madrid, Spain*
- ³²*Massachusetts Institute of Technology, Cambridge, Massachusetts 02139*
- ³³*Institute of Particle Physics: McGill University, Montréal, Canada H3A 2T8; and University of Toronto, Toronto, Canada M5S 1A7*
- ³⁴*University of Michigan, Ann Arbor, Michigan 48109*
- ³⁵*Michigan State University, East Lansing, Michigan 48824*
- ³⁶*Institution for Theoretical and Experimental Physics, ITEP, Moscow 117259, Russia*
- ³⁷*University of New Mexico, Albuquerque, New Mexico 87131*
- ³⁸*Northwestern University, Evanston, Illinois 60208*
- ³⁹*The Ohio State University, Columbus, Ohio 43210*
- ⁴⁰*Okayama University, Okayama 700-8530, Japan*
- ⁴¹*Osaka City University, Osaka 588, Japan*
- ⁴²*University of Oxford, Oxford OX1 3RH, United Kingdom*
- ⁴³*University of Padova, Istituto Nazionale di Fisica Nucleare, Sezione di Padova-Trento, I-35131 Padova, Italy*
- ⁴⁴*LPNHE, Universite Pierre et Marie Curie/IN2P3-CNRS, UMR7585, Paris, F-75252 France*
- ⁴⁵*University of Pennsylvania, Philadelphia, Pennsylvania 19104*
- ⁴⁶*Istituto Nazionale di Fisica Nucleare Pisa, Universities of Pisa, Siena and Scuola Normale Superiore, I-56127 Pisa, Italy*
- ⁴⁷*University of Pittsburgh, Pittsburgh, Pennsylvania 15260*
- ⁴⁸*Purdue University, West Lafayette, Indiana 47907*
- ⁴⁹*University of Rochester, Rochester, New York 14627*
- ⁵⁰*The Rockefeller University, New York, New York 10021*
- ⁵¹*Istituto Nazionale di Fisica Nucleare, Sezione di Roma 1, University of Rome "La Sapienza," I-00185 Roma, Italy*
- ⁵²*Rutgers University, Piscataway, New Jersey 08855*
- ⁵³*Texas A&M University, College Station, Texas 77843*
- ⁵⁴*Istituto Nazionale di Fisica Nucleare, University of Trieste/ Udine, Italy*
- ⁵⁵*University of Tsukuba, Tsukuba, Ibaraki 305, Japan*
- ⁵⁶*Tufts University, Medford, Massachusetts 02155*
- ⁵⁷*Waseda University, Tokyo 169, Japan*
- ⁵⁸*Wayne State University, Detroit, Michigan 48201*
- ⁵⁹*University of Wisconsin, Madison, Wisconsin 53706*
- ⁶⁰*Yale University, New Haven, Connecticut 06520*

Using 355 pb^{-1} of data collected by the CDF II detector in $p\bar{p}$ collisions at $\sqrt{s} = 1.96 \text{ TeV}$ at the Fermilab Tevatron, we study the fully reconstructed hadronic decays $B_{(s)}^0 \rightarrow D_{(s)}^- \pi^+$ and $B_{(s)}^0 \rightarrow D_{(s)}^- \pi^+ \pi^+ \pi^-$. We present the first measurement of the ratio of branching fractions $\mathcal{B}(B_s^0 \rightarrow D_s^- \pi^+ \pi^+ \pi^-) / \mathcal{B}(B^0 \rightarrow D^- \pi^+ \pi^+ \pi^-) = 1.05 \pm 0.10(\text{stat.}) \pm 0.22(\text{syst.})$. We also update our measurement of $\mathcal{B}(B_s^0 \rightarrow D_s^- \pi^+) / \mathcal{B}(B^0 \rightarrow D^- \pi^+)$ to $1.13 \pm 0.08(\text{stat.}) \pm 0.23(\text{syst.})$ improving the statistical uncertainty by more than a factor of two. We find $\mathcal{B}(B_s^0 \rightarrow D_s^- \pi^+) = [3.8 \pm 0.3(\text{stat.}) \pm 1.3(\text{syst.})] \times 10^{-3}$ and $\mathcal{B}(B_s^0 \rightarrow D_s^- \pi^+ \pi^+ \pi^-) = [8.4 \pm 0.8(\text{stat.}) \pm 3.2(\text{syst.})] \times 10^{-3}$.

PACS numbers: 13.25.Hw 14.40.Nd

Hadronic B meson decays provide important information on both weak and hadronic interactions of heavy flavored mesons. The dominant hadronic decay modes of the B meson involve tree-level diagrams where the $b \rightarrow c$ transition leads to a charmed meson and a vir-

tual W boson, which often emerges as a charged π, ρ , or $a_1(1260)$ meson [1]. The measurement of the ratios of branching fractions $\mathcal{B}(B_s^0 \rightarrow D_s^- \pi^+ [\pi^+ \pi^-]) / \mathcal{B}(B^0 \rightarrow D^- \pi^+ [\pi^+ \pi^-])$ [2] reveals information about B decay mechanisms. One can attempt to separate the con-

tributions of various processes in $B^0 \rightarrow D^- \pi^+$ decay and then predict $B_s^0 \rightarrow D_s^- \pi^+$ branching fraction using SU(3)[3, 4], and further estimate flavor SU(3) symmetry breaking effects [5], which can be sizable [6].

Experimentally the sample of $B_s^0 \rightarrow D_s^- \pi^+ \pi^+ \pi^-$ decays is included in the data set used for the first measurement of the B_s^0 oscillation frequency [7]. In this letter we present the first measurement of the ratio of branching fractions $R(D3\pi) = \mathcal{B}(B_s^0 \rightarrow D_s^- \pi^+ \pi^+ \pi^-) / \mathcal{B}(B^0 \rightarrow D^- \pi^+ \pi^+ \pi^-)$ using D_s^- decays to $\phi\pi^-$, $K^{*0}K^-$, $\pi^-\pi^-\pi^+$, and D^- decays to $K^+\pi^-\pi^-$. We also update our previous [8] measurement of the ratio $R(D\pi) = \mathcal{B}(B_s^0 \rightarrow D_s^- \pi^+) / \mathcal{B}(B^0 \rightarrow D^- \pi^+)$. We measure the ratios of branching fractions because most of the systematic uncertainties cancel due to the similarity of final state kinematics. In addition, some common theoretical factors [9] also cancel in taking the ratio. The measurement is performed using a sample of inclusive heavy flavor decays selected by the displaced track trigger described below, corresponding to an integrated luminosity of 355 pb^{-1} of $p\bar{p}$ collisions at $\sqrt{s} = 1.96 \text{ TeV}$.

The components of the CDF II detector relevant for this analysis are briefly described below. A more complete description can be found elsewhere [10]. Charged particle tracks are reconstructed in the pseudo-rapidity range $|\eta| \lesssim 1.0$, where η is defined as $-\ln \tan(\theta/2)$, and θ represents the angle between the particle and the proton beam direction [11]. Tracks are reconstructed from hits in the silicon microstrip detector (SVX) and the central outer tracker (COT). Both detectors are inside a 1.4 T solenoidal magnetic field. The SVX detector is composed of L00 (single layer of silicon placed close to the beam pipe), SVX II (five cylindrical layers of double-sided sensors), and ISL (outermost layer of silicon), providing up to 8 coordinate measurements in the r - ϕ view [12]. Surrounding the SVX is the COT, an open cell drift chamber with 96 layers of sense wires [13]. A sample rich in charm and beauty hadrons is selected by a three-level displaced track trigger. At level 1, tracks are reconstructed in the COT by the track trigger processor (XFT) [14]. The trigger requires two tracks with transverse momenta $p_T > 2 \text{ GeV}/c$ and the scalar sum $p_{T1} + p_{T2} > 4.0 \text{ GeV}/c$. The level 2 silicon vertex tracker (SVT) [15] associates SVX II r - ϕ position measurements with XFT tracks, providing a precise measurement of the track impact parameter (d_0), i.e. the distance of closest approach of the track helix to the beam axis in the transverse plane. Decays of heavy flavor particles are identified by requiring two tracks with $0.12 \text{ mm} < d_0 < 1 \text{ mm}$ and an opening angle in the transverse plane $2^\circ < |\Delta\phi| < 90^\circ$. A requirement $L_{xy} > 0.2 \text{ mm}$ is also applied, where L_{xy} is defined as the distance in the transverse plane from the beam line to the two-track vertex projected onto the two-track momentum vector. The level 3 trigger receives the complete detector information and performs a full event reconstruction applying selection similar to level 1 and level 2 on offline quality

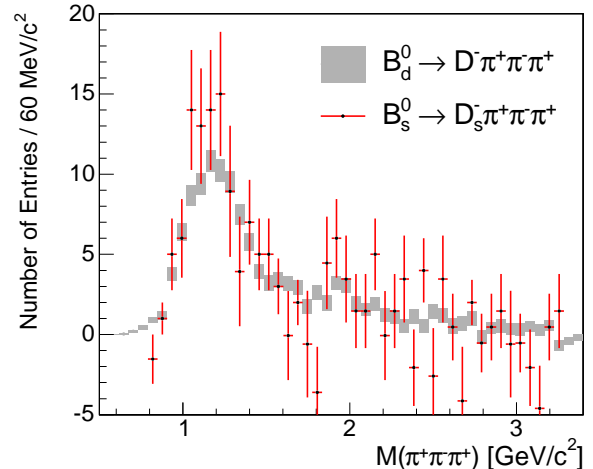


FIG. 1: Comparison of the sideband subtracted mass spectrum of $\pi^+\pi^+\pi^-$ from B^0 and B_s^0 decays. Only the $D_s^- \rightarrow \phi\pi$ channel is used for B_s^0 . The B^0 histogram is normalized to B_s^0 .

quantities.

B candidate reconstruction starts with a collection of tracks. No particle identification is explicitly used, and tracks are assumed to be either a pion or kaon to match the reconstruction hypothesis. A set of unique track combinations making the ϕ , K^{*0} , D^- , D_s^- , and B candidates is formed. The track combinations reconstructed in 3 dimensions must be consistent with forming a vertex, and combinations that fall outside a wide mass window around the mass of the respective meson are rejected.

The Monte Carlo simulation is an essential part of this analysis. It is used to optimize the selection cuts, model signal and background, and to study the trigger and reconstruction efficiency. We generate single B hadrons with the program BGENERATOR[16]. The B -hadron decays are simulated with EVTGEN [17]. This package has been extensively tuned by experiments at the $\Upsilon(4S)$ resonance and reflects the measured properties of B and D meson decays. The simulation is validated by comparing kinematic quantities of the decays and quantities relevant for the trigger selection with data.

The selection requirements used to reject combinatorial background are optimized by maximizing $S/\sqrt{S+B}$ for each mode individually. The number of signal events (S) is derived from a Monte Carlo simulation of the CDF II detector and trigger. The number of background events (B) is estimated using data in the high-mass sideband interval, $m(B) + 10 \sigma(B)$ to $m(B) + 16 \sigma(B)$, where $m(B)$ is the fitted mass and $\sigma(B) \approx 15 \text{ MeV}/c^2$ is the width of the signal peak. This sideband represents the combinatoric background underneath the signal peak. Selection requirements include cuts on the impact parameter of the B meson, the $\chi_{\tau-\phi}^2$ [18] of the B vertex

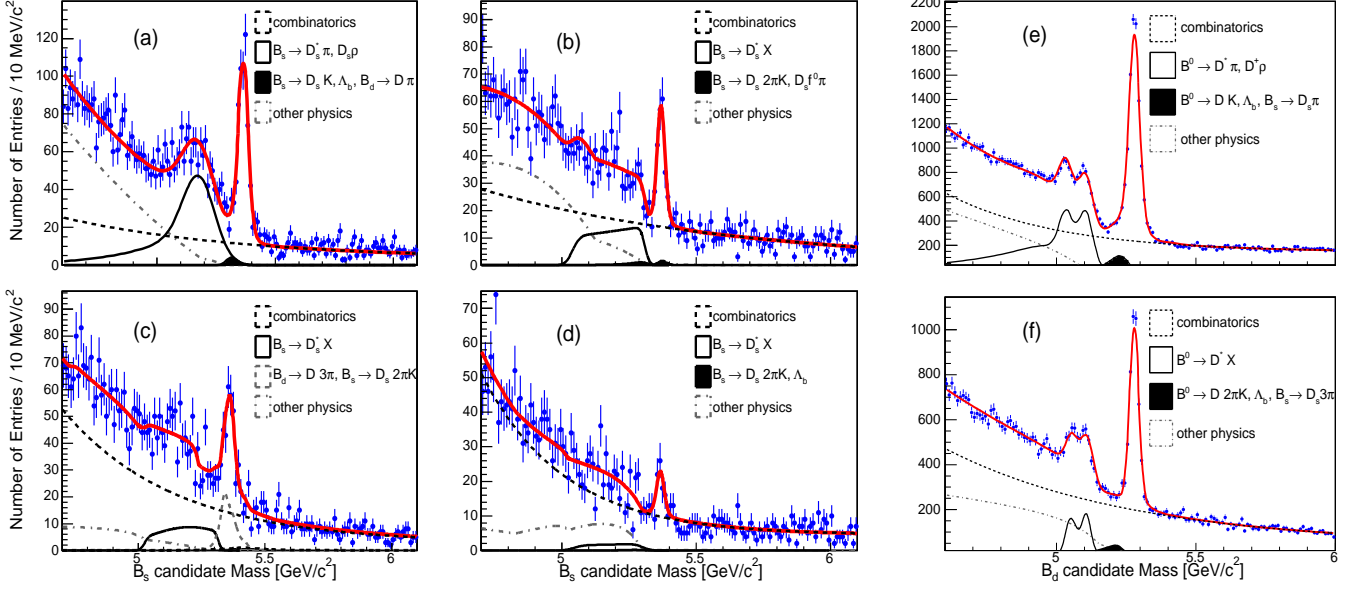


FIG. 2: Mass spectra for (a) $B_s^0 \rightarrow D_s^- \pi^+$ (b) $B_s^0 \rightarrow D_s^- (\phi \pi^-) \pi^+ \pi^+ \pi^-$ (c) $B_s^0 \rightarrow D_s^- (K^{*0} K^-) \pi^+ \pi^+ \pi^-$ (d) $B_s^0 \rightarrow D_s^- (\pi^- \pi^- \pi^+) \pi^+ \pi^+ \pi^-$ (e) $B^0 \rightarrow D^- \pi^+$ (f) $B^0 \rightarrow D^- \pi^+ \pi^+ \pi^-$. The “other physics” category corresponds to the inclusive $B \rightarrow D_s^- X$ and $B \rightarrow D^- X$ decays.

fit in the transverse plane, the p_T of the pion from the B decay in $B_{(s)}^0 \rightarrow D_{(s)}^- \pi^+$, and a minimum p_T requirement of the tracks for decays with 6 tracks in the final state. We exploit the narrow $\phi \rightarrow K^+ K^-$ resonance and $K^{*0} \rightarrow K^+ \pi^-$ resonance to suppress background by requiring $1010 \text{ MeV}/c^2 < m(\phi) < 1029 \text{ MeV}/c^2$ and $840 \text{ MeV}/c^2 < m(K^{*0}) < 940 \text{ MeV}/c^2$. There are also requirements on $L_{xy}/\sigma(L_{xy})$ - the significance of the measurement of L_{xy} for B and D vertices.

The assumptions on the relative contributions of resonant $a_1, \rho\pi$, and non-resonant $\pi^+ \pi^+ \pi^-$ in the $B^0 \rightarrow D^- \pi^+ \pi^+ \pi^-$ signal affect $R(D3\pi)$ because Monte Carlo simulation shows that their reconstruction efficiencies differ. We find that the contribution of the a_1 resonance is dominant. The $\pi^+ \pi^+ \pi^-$ mass distributions were compared in data between B^0 and B_s^0 mesons and are compatible within statistics, as shown in Fig.1. The resonant fractions in $B_s^0 \rightarrow D_s^- \pi^+ \pi^+ \pi^-$ and $B^0 \rightarrow D^- \pi^+ \pi^+ \pi^-$ decays are assumed to be identical.

To extract $R(D3\pi)$ (or equivalently $R(D\pi)$), we follow the general procedure described in Ref. [8], using the following formula:

$$R(D3\pi) = \frac{f_d}{f_s} \cdot \frac{\epsilon(B^0)}{\epsilon(B_s^0)} \cdot \frac{\mathcal{B}(D^-)}{\mathcal{B}(D_s^-)} \cdot \frac{N(B_s^0)}{N(B^0)}, \quad (1)$$

where $N(B_s^0)$ and $N(B^0)$ are the measured signal yields, $\epsilon(B^0)/\epsilon(B_s^0)$ is the ratio of trigger and reconstruction efficiencies extracted from Monte Carlo simulation, f_d/f_s is the ratio of b quark fragmentation fractions into B^0 and B_s^0 mesons, and $\mathcal{B}(D^-)/\mathcal{B}(D_s^-)$ is the ratio of the

world average values for branching fractions of D^- and D_s^- mesons into the reconstructed final states [19].

The yields, $N(B_s^0)$ and $N(B^0)$, are extracted from the mass spectra in Fig.2 using a binned likelihood fit and are summarized in Table I. In the normalization modes $B^0 \rightarrow D^- \pi^+$ and $B^0 \rightarrow D^- \pi^+ \pi^+ \pi^-$ we observe $8098 \pm 114(\text{stat.})$ and $3288 \pm 76(\text{stat.})$ signal candidates respectively. The signal peaks are modeled with a sum of two Gaussians with the same mean values but different widths. We follow the treatment of backgrounds as done in Ref. [8]. The combinatorial background is modeled with a sum of an exponential function and a constant. The shapes of other physics backgrounds are modeled using Monte Carlo simulation, and their parameterization is fixed in the fits to the mass spectra.

For B^0 meson candidates, the structure below the main B peak has two pronounced peaks. This structure is the result of a $B^0 \rightarrow D^{*-} \pi^+ (\pi^+ \pi^+ \pi^-)$ decay followed by a $D^{*-} \rightarrow D^- \pi^0$ decay. Angular momentum conservation in B decay implies a spin alignment of the D^{*-} that, combined with the low Q value of its decay, leads to the two distinct peaks in the $D^- \pi^+ (\pi^+ \pi^+ \pi^-)$ mass distribution seen in the data. In the case of the analogous $B_s^0 \rightarrow D_s^{*-} \pi^+ \pi^+ \pi^-$ decay, the D_s^{*-} decays to D_s^- and a photon 94% of the time [19]. This produces a single, relatively broad structure as seen in our data. None of these backgrounds contribute under the signal peak.

There are several backgrounds whose mass distributions peak near the signal region and must be subtracted. They are the Cabibbo suppressed decays $B_{(s)}^0 \rightarrow D_{(s)}^- K^+$

Decay	Yield	$\epsilon(B_s^0)/\epsilon(B^0)$	$\mathcal{B}(D^-)/\mathcal{B}(D_s^-)$	$f_s/f_d \cdot BR(B_s^0)/BR(B^0)$
$D_s^- (\phi\pi^-)\pi^+$	494 ± 28	0.913 ± 0.004	4.40 ± 0.59	$0.292 \pm 0.020(stat) \pm 0.012(syst)$
$D_s^- (\phi\pi^-)\pi^+\pi^+\pi^-$	160 ± 17	0.814 ± 0.010	4.40 ± 0.59	$0.263 \pm 0.029(stat) \pm 0.018(syst)$
$D_s^- (K^*K^-)\pi^+\pi^+\pi^-$	90 ± 17	0.352 ± 0.009	3.80 ± 0.77	$0.274 \pm 0.053(stat) \pm 0.030(syst)$
$D_s^- (\pi^-\pi^+\pi^-)\pi^+\pi^+\pi^-$	49 ± 11	0.397 ± 0.009	7.80 ± 1.50	$0.293 \pm 0.067(stat) \pm 0.021(syst)$

TABLE I: Summary of event yields, ratios of efficiencies, and individual branching ratio measurements. The uncertainties listed on the yield and the ratio of efficiencies are statistical only. $\mathcal{B}(D^-)/\mathcal{B}(D_s^-)$ is the ratio of $\mathcal{B}(D^- \rightarrow K^+\pi^-\pi^-)$ to the corresponding branching fraction of the D_s^- meson ($\mathcal{B}(D_s^- \rightarrow \phi\pi^-, \phi \rightarrow K^-K^+)$, $\mathcal{B}(D_s^- \rightarrow K^{*0}K^-, K^{*0} \rightarrow K^-\pi^+)$ or $\mathcal{B}(D_s^- \rightarrow \pi^-\pi^+\pi^-)$).

and $B_{(s)}^0 \rightarrow D_{(s)}^- K^+ \pi^- \pi^+$, and mis-reconstructed baryon decays $\Lambda_b^0 \rightarrow \Lambda_c^+ \pi^-$ and $\Lambda_b^0 \rightarrow \Lambda_c^+ \pi^- \pi^+ \pi^-$. The ratio of Cabibbo-suppressed $B_{(s)}^0 \rightarrow D_{(s)}^- K^+$ background to the corresponding signal was fixed to the world average ratio of branching fractions [19]. The ratio of Cabibbo-suppressed $B_{(s)}^0 \rightarrow D_{(s)}^- K^+ \pi^- \pi^+$ decay to the signal is fixed to $\frac{|V_{us}|^2}{|V_{ud}|^2} \approx 0.05$. The fraction of Λ_b background was fixed using the recent CDF measurement of $\mathcal{B}(\Lambda_b^0 \rightarrow \Lambda_c^+ \pi^-)/\mathcal{B}(B^0 \rightarrow D^- \pi^+)$ [20]. In all the cases, the ratios are corrected for the relative trigger and reconstruction efficiencies.

In the case of the $B_s^0 \rightarrow D_s^- \pi^+ \pi^+ \pi^-$ decay, there is a reflection from $B^0 \rightarrow D^- \pi^+ \pi^+ \pi^-$. If one of the pions from a $D^- \rightarrow K^+ \pi^- \pi^-$ decay is reconstructed as a kaon, a peak is produced under the B_s^0 signal region. These events contribute in the $B_s^0 \rightarrow D_s^- \pi^+ \pi^+ \pi^-$, $D_s^- \rightarrow K^{*0} K^-$ decay because the K^{*0} resonance is broad. The fraction of $B^0 \rightarrow D^- \pi^+ \pi^+ \pi^-$ events under $B_s^0 \rightarrow D_s^- \pi^+ \pi^+ \pi^-$ peaks is calculated from the observed number of B^0 mesons. The number of $B^0 \rightarrow D^- \pi^+ \pi^+ \pi^-$ events under the $B_s^0 \rightarrow D_s^- (K^{*0} K^-) \pi^+ \pi^+ \pi^-$ mass distribution is estimated to be $141 \pm 6(stat.)$. The systematic uncertainty assigned due to the $B^0 \rightarrow D^- \pi^+ \pi^+ \pi^-$ background subtraction is dominant in this channel and is a part of the “ B_s^0 fit model” (see Table II). For $B_s^0 \rightarrow D_s^- \pi^+ \pi^+ \pi^-$ with $D_s^- \rightarrow \phi\pi^-$ the corresponding B^0 background fraction is very small due to the narrow width of the ϕ . The contamination of the double charm $B^0 \rightarrow D^- D_s^+$, with $D_s^+ \rightarrow \pi^+ \pi^- \pi^+$, is estimated to be $\approx 1\%$ of the $B^0 \rightarrow D^- \pi^+ \pi^+ \pi^-$ signal and is subtracted from the measured yield. The contamination of $B_s^0 \rightarrow D_s^- D_s^+$ in the B_s^0 signal is found to be negligible. Applying a cut on the mass of three pions in the $B_s^0 \rightarrow D_s^- \pi^+ \pi^+ \pi^-$ decay around the mass of the D_s^- meson does not change the measured yields.

Systematic uncertainties due to the fitting procedure are estimated by comparing the fitted yields after changing the mass range in which the fit is performed and also by varying the parameters of functions describing the backgrounds. The systematic uncertainty on the ratio of efficiencies $\epsilon(B_s^0)/\epsilon(B^0)$ comes from various physics sources. In all cases, the systematics were estimated by observing the change in the ratio of efficien-

cies when the effect was considered. The effect of the choice of B meson spectrum used by Monte Carlo simulation was determined by reweighting the Monte Carlo events with p_T spectrum based on NLO calculations [16] to match the p_T spectrum measured at CDF [21]. To estimate the systematic uncertainty due to B and D lifetimes we varied the assumed lifetime of B and D meson in signal Monte Carlo within world average values [19]. The composition systematic applies to the decay $B_s^0 \rightarrow D_s^- (\pi^-\pi^+\pi^-)\pi^+\pi^+\pi^-$ only and is due to the limited knowledge of the resonances in $D_s^- \rightarrow \pi^-\pi^+\pi^-$ decay. We assign a systematic uncertainty due to the unknown resonance structure of the $\pi^+\pi^+\pi^-$ system in $B_{(s)}^0 \rightarrow D_{(s)}^- \pi^+\pi^+\pi^-$ decay by varying the fraction of a_1 component in both B^0 and B_s^0 signal Monte Carlo in a range consistent with the observed shape. The systematic uncertainties are summarized in Table II.

The results of the measurements for $R(D3\pi)$ are summarized in Table I. To average the results of the measurements by the expected yield we use Eq.(1), where $N(B_s^0)$ is a sum of the yields in three B_s^0 channels and $\epsilon(B_s^0)$ is a linear combination of Monte Carlo efficiencies multiplied by the ratio of the branching fraction of D_s^- decay in a given channel and $\mathcal{B}(D_s^- \rightarrow \phi\pi)$. Using $f_s/f_d = 0.259 \pm 0.038$ [19], we obtain:

$$R(D3\pi) = 1.05 \pm 0.10(stat.) \pm 0.07(syst.) \pm 0.14(br) \pm 0.15(pr)$$

The (br) and (pr) uncertainties refer to the uncertainty on the D meson branching fractions and the ratio of fragmentation fractions f_s/f_d .

Using Eq.(1) and the input from Table I, we obtain:

$$R(D\pi) = 1.13 \pm 0.08(stat.) \pm 0.05(syst.) \pm 0.15(br) \pm 0.17(pr)$$

The measurement of $R(D\pi)$ is consistent with the previous CDF measurement [8] and supersedes that result with a statistical uncertainty reduced by a factor of two. This measurement is consistent within uncertainties with the theoretical prediction of 1.05 ± 0.24 [3].

In conclusion, we have presented the first measurement of the ratio of branching fractions $R(D3\pi)$. We also have measured the ratio of branching fractions $R(D\pi)$ improving the statistical uncertainty by more than a factor of two. Using the world average values for $\mathcal{B}(B^0 \rightarrow$

$D^- \pi^+$) and $\mathcal{B}(B^0 \rightarrow D^- \pi^+ \pi^+ \pi^-)$ [19] we find $\mathcal{B}(B_s^0 \rightarrow D_s^- \pi^+) = [3.8 \pm 0.3(\text{stat.}) \pm 1.3(\text{syst.})] \times 10^{-3}$ and $\mathcal{B}(B_s^0 \rightarrow D_s^- \pi^+ \pi^+ \pi^-) = [8.4 \pm 0.8(\text{stat.}) \pm 3.2(\text{syst.})] \times 10^{-3}$.

Effect	Syst. Uncertainty[%]	
	$B \rightarrow D\pi$	$B \rightarrow D3\pi$
B p_T spectrum	± 3.0	± 3.0
B_s^0 lifetime	± 2.1	± 2.1
3π resonance structure	n/a	± 2.5
$D_s^- \rightarrow 3\pi$ composition	n/a	± 3.0
trigger simulation	± 1.2	± 1.1
B^0 fit model	± 0.5	± 1.3
B_s^0 fit model	± 1.5	$\pm(3.6 - 9.3)$
Total	± 4.2	$\pm(6.7 - 10.9)$

TABLE II: Summary of the relative systematics uncertainties on $R(D\pi)$ and $R(D3\pi)$. The range of values appearing in the second column reflects the differences in the fit systematic of the three B_s^0 decays.

We thank the Fermilab staff and the technical staffs of the participating institutions for their vital contributions. This work was supported by the U.S. Department of Energy and National Science Foundation; the Italian Istituto Nazionale di Fisica Nucleare; the Ministry of Education, Culture, Sports, Science and Technology of Japan; the Natural Sciences and Engineering Research Council of Canada; the National Science Council of the Republic of China; the Swiss National Science Foundation; the A.P. Sloan Foundation; the Bundesministerium für Bildung und Forschung, Germany; the Korean Science and Engineering Foundation and the Korean Research Foundation; the Particle Physics and Astronomy Research Council and the Royal Society, UK; the Russian Foundation for Basic Research; the Comisión Interministerial de Ciencia y Tecnología, Spain; in part by the European Community's Human Potential Programme under contract HPRN-CT-2002-00292; and the Academy of Finland.

-
- [1] H. J. Lipkin, Phys. Lett. B **515**, 81 (2001).
 - [2] Reference to the charge-conjugate decays is implied here and throughout the text.
 - [3] P. Colangelo and R. Ferrandes, Phys. Lett. B **627**, 77 (2005).
 - [4] A. K. Leibovich, Z. Ligeti, I.W. Stewart, and M.B. Wise, Phys. Lett. B **586**, 337(2004).
 - [5] C.S. Kim, S. Oh, and C. Yu, Phys. Lett. B **621**, 259 (2005).
 - [6] Z. Z. Xing, High Energy Phys. Nucl. Phys. **26**, 100 (2002).
 - [7] A. Abulencia *et al.* (CDF Collaboration), Phys. Rev.Lett. **97**, 062003 (2006).
 - [8] A. Abulencia *et al.* (CDF Collaboration), Phys. Rev.Lett. **96**, 191801 (2006).
 - [9] A. Leibovich, private communication.
 - [10] D. Acosta *et al.* (CDF Collaboration), Phys. Rev. D **71**, 032001 (2005).
 - [11] CDF II uses a cylindrical coordinate system in which ϕ is an azimuthal angle, r is the radius from the symmetry axis, y points up, and z points in the proton beam direction with the origin at the center of the detector. The transverse plane is the plane perpendicular to the z axis.
 - [12] A. Sill *et al.*, Nucl. Instrum. Meth. **A 447**, 1 (2000).
 - [13] T. Affolder *et al.*, Nucl. Instrum. Meth. **A 526**, 249 (2004).
 - [14] E.J. Thomson *et al.*, IEEE Trans. Nucl. Sci. **49**, 1063 (2003).
 - [15] W. Ashmanskas *et al.*, Nucl. Instrum. Meth. **A 518**, 532 (2004)
 - [16] P. Nason, S. Dawson, and R.K. Ellis, Nucl. Phys. B **303** 607 (1988); Nucl. Phys. B **327**, 49 (1989).
 - [17] D. Langle, Nucl. Meth. in Phys. Res. A **462**, 152 (2001).
 - [18] $\chi_{r-\phi}^2$ is a χ^2 -like goodness-of-fit quantity using only the track parameters in the transverse plane.
 - [19] W.-M. Yao *et al.* (Particle Data Group), J. Phys. G **33**, 1 (2006).
 - [20] A. Abulencia *et al.* (CDF Collaboration), arXiv:hep-ex/0601003.
 - [21] D. Acosta *et al.* (CDF Collaboration), Phys. Rev. D **71**, 032001 (2005).